# Deoxynucleic Guanidine/Peptide Nucleic Acid Chimeras: Synthesis, Binding and Invasion Studies with DNA

**Dinesh A. Barawkar,[†] Yan Kwok,[‡] Thomas W. Bruice,[‡] and Thomas C. Bruice*[,†]**

*Contribution from the Department of Chemistry and Biochemistry, University of California, Santa Barbara, California 93106, and Department of Biochemistry and Biophysics, Genelabs Technologies, Inc., 505 Penobscot Drive, Redwood City, California 94063*

*Received January 3, 2000*

**Abstract:** A fully automated solid-phase synthetic procedure for incorporation of positively charged guanidinium linkages into otherwise neutral PNA sequences has been employed. These DNG/PNA chimeras form [(DNG/PNA)$_2$·DNA] triplexes upon binding to single strand or duplex DNA (with accompanying D-loop for the latter). The [(DNG/PNA)$_2$·DNA] triplexes of DNG/PNA $T_{10}$, with DNA $dA_{10}$, are more stable than DNA·DNA triplexes [$(T_{10})_2$·$dA_{10}$]. The binding of DNG/PNA chimera with guanidinium linkages on both ends, with single strand length-matched complementary DNA under thermal melt conditions and with longer double strand DNA under isothermal conditions is sequence specific. The association process of DNG/PNA chimera with single strand DNA and strand invasion of longer ds-DNA is faster than the association of PNA, with the same DNA targets, as evident by thermal hysteresis and gel retardation under isothermal conditions. The sequence specific and faster strand invasion of DNG/PNA may extend the potential utility of PNA in diagnostics, biomolecular probes, and antisense/antigene therapeutics.

## Introduction

To identify oligonucleotide (ODN) analogues that would serve as effective antisense, antigene, and experimental agents, considerable attention[1−3] has been paid to the modification of DNA and RNA. The affinity and kinetics of hybridization of DNA and RNA helices are attenuated due to electrostatic repulsion of the negative charges on adjacent backbone phosphodiester linkages. The phosphodiester linkage is also responsible for low cellular uptake as well as the degradation of ODNs by nucleases. The negative charge−charge repulsion can be minimized or eliminated if the negatively charged phosphodiester linkages are replaced by uncharged[4,5] or positively charged linkages,[6−12] or by the use of oligonucleotide conjugates with positively charged groups to provide zwitterionic DNA analogues.[13−15]

Peptide nucleic acid polymers (PNA) have internucleobase linkages which are uncharged (Scheme 1). The favorable PNA structure and lack of electrostatic repulsion between PNA and its DNA/RNA targets result in their high binding affinity.[16] However, the prospect of PNAs as drugs has limitations, such as poor solubility and cell membrane permeability,[17,18] small rate constants for association with DNA and RNA,[19,20] and the high thermal stability of helical PNA:DNA or PNA:RNA structures which may lead to decreased sequence specificity at physiological temperature.[21] As PNA is achiral, the unrestrained polyamide backbone of the PNA binds to its DNA/RNA targets in both parallel (N-PNA/5′-DNA) and antiparallel (N-PNA/3′-DNA) orientations.[22]

An attempt to increase the rate of PNA association with DNA, as well as to increase its solubility in aqueous medium, involved introduction of positive charges in PNA. Covalent conjugation of spermine at the C-terminus of PNA[23] resulted in stabilization

[†] University of California, Santa Barbara.

[‡] Genelabs Technologies, Inc.

(1) De Mesmaeker, A.; Haner. R.; Martin, P.; Moser, H. E. *Acc. Chem. Res*. **1995**, *28*, 366−374.

(2) Milligan, J. F.; Matteucci, M. D.; Martin, C. J. *J. Med. Chem.***1993**, *36*, 1923−1937.

(3) Sanghvi, Y. S.; Cook, P. D. In *Nucleosides and Nucleotides as Antitumor and Antiviral Agents*, Chu, C. K, Baker, D. C., Eds.; Plenum Press: New York, 1993; p 311.

(4) Nielsen, P.; Egholm, M.; Berg, R. H.; Buchardt, O. *Science* **1991**, *254*, 1497−1500.

(5) Kean, J. M.; Kipp, S. A.; Miller, P. S.; Kulka, M.; Aurelian, L. *Biochemistry* **1995**, *34*, 14617−14620.

(6) Dempcy, R. O.; Browne, K. A.; Bruice, T. C. *J. Am. Chem. Soc.* **1995**, *117*, 6140−6141.

(7) Dempcy, R. O.; Luo, J.; Bruice, T. C. *Proc. Natl. Acad. Sci. U.S.A.* **1996**, *93*, 4326−4330.

(8) Linkletter, B.; Szabo, I. E.; Bruice, T. C. *J. Am. Chem. Soc.* **1999**, *121*, 3888−3896.

(9) Arya, D. P.; Bruice, T. C. *J. Am. Chem. Soc*. **1999**, *120*, 12419−12427.

(10) Barawkar, D. A.; Bruice, T. C. *Proc. Natl. Acad. Sci. U.S.A.* **1998**, *95*, 11047−11052.

(11) Letsinger, R. L.; Singman, C. N.; Histand, G.; Salunkhe, M. *J. Am. Chem. Soc*. **1988** *110*, 4470−4471.

(12) Fathi, R.; Huang, Q.; Coppola, G.; Delaney, W.; Teasdale, R.; Krieg, A. M.; Cook, A. F. *Nucleic Acids Res.* **1994**, *22*, 5416−5424.

(13) Barawkar, D. A.; Rajeev, K. G.; Kumar, V. A.; Ganesh, K. N. *Nucleic Acids Res.* **1996**, *24*, 1229−1237.

(14) Hashimoto, H.; Nelson, M. G.; Switzer, C. J. *J. Am. Chem. Soc.* **1993**, *115*, 7128−7134.

(15) Schmid N.; Behr, J. P. *Tetrahedron Lett*. **1995**, *36*, 1447−1450.

(16) Hyrup, B.; Nielsen, P. E. *Bioorg. Med. Chem.* **1996**, *4*, 5−23.

(17) Buchardt, O.; Egholm, M.; Berg, R. H.; Nielsen, P. E. *TIBTECH* **1993**, *11*, 384−386.

(18) Wittung, P.; Kajanus, J.; Edwards, K.; Nielsen, P.; Norden, B.; Malmstrom, B. G. *FEBS Lett.* **1995**, *365*, 27−29.

(19) Griffith, M. C.; Risen, L. M.; Grieg, M. J.; Lesnik, E. A.; Sprankle, K. G.; Griffey, R. H.; Kiely, J. S.; Frier, S. M. *J. Am. Chem. Soc*. **1995**, *117*, 831−832.

(20) Kuhn, H.; Demidov, V. V.; Frank-Kamenetskii, M. D.; Nilesen, P. E. *Nucleic Acids Res.* **1998**, *26*, 582−587.

(21) Meier, C.; Engels, J. W. *Angew. Chem., Int. Ed. Engl.* **1992**, *31*, 1008−1010.

(22) Peffer, N. J.; Hanvey, J. C.; Bisi, J. E.; Thomson, S. A.; Hassman, C. F.; Noble, S. A.; Babiss, L. E. *Proc. Natl. Acad. Sci. U.S.A.* **1993**, *90*, 10648−10652.

10.1021/ja000022l CCC: $19.00 
Published on Web 05/20/2000

**Scheme 1**

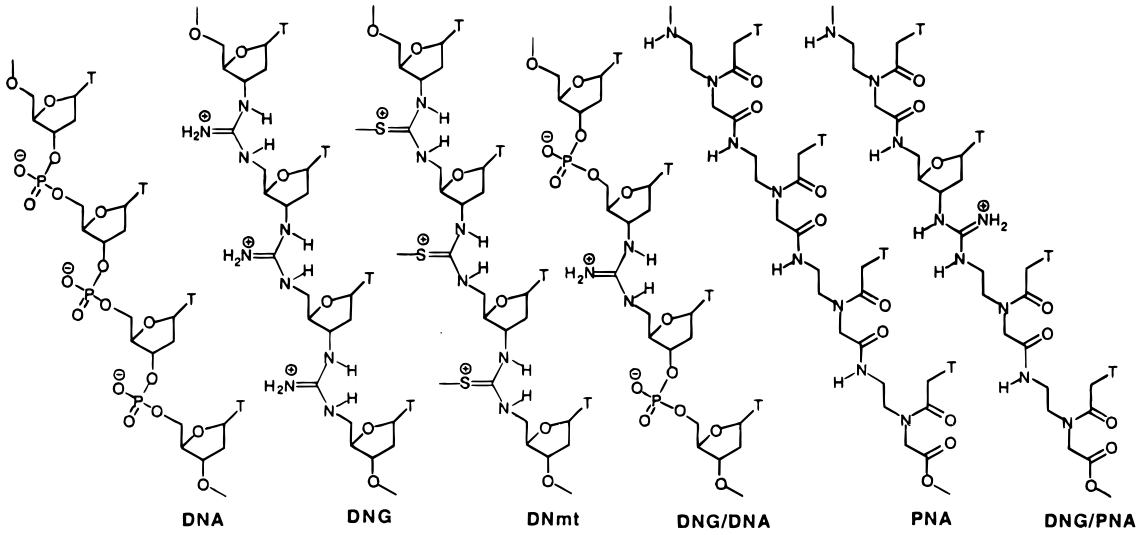


of the PNA·DNA and $(PNA)_2$·DNA structures. Similarly, linking two PNA molecules with a positively charged lysine$_3$/aminohexyl$_2$ linker[19] provided faster rates of association and more stable PNA·DNA triplexes than mono PNA. Introduction of positive charge at the branch point of the PNA backbone by replacement of a nucleobase linker amide with a tertiary amine caused a large destabilization of PNA·DNA duplexes and $(PNA)_2$·DNA triplexes.[24] Incorporation of chirality into PNA, to provide discrimination between parallel and antiparallel binding orientations has been studied by: (i) synthesis of PNA/peptide[25] and PNA/DNA[26] chimeras, (ii) replacement of the glycine unit in the PNA backbone with chiral amino acids,[27] as in the incorporation of three D-lysine units in the backbone of a 10-mer PNA, which resulted in better binding to an antiparallel DNA target than to parallel DNA, and (iii) placing conformational constraints on the PNA structure by bridging the methylene group between $\beta$-C of the aminoethyl unit with the $\alpha$-C of the glycyl unit of PNA, to generate the chiral 4-aminoprolyl backbone.[28] The presence of even one chiral 4-aminoprolyl unit in a PNA backbone, either at the N-terminus or at an internal site, confers the ability to bind in only one orientation with target DNA.

Our ongoing research in this area is focused on the development of positively charged internucleoside linkages[6−9] which provide stabilized complexes with DNA or RNA.[29,30] In these studies the $-O-(PO_2^-)-O-$ linkers are replaced (Scheme 1) either by $-NH-C(=NH_2^+)-NH-$, to provide deoxynucleic guanidines (DNG),[6−8] or by $-NH-C(=S^+CH_3)-NH-$, to provide *S*-methylthiourea-nucleosides (DNmt).[9] Annealing and melting studies have shown that double and triple helices between DNG or DNmt and DNA are formed with fidelity of nucleobase recognition.[6−9] However, the sequence nonspecific electrostatic attractive forces between DNA or RNA and DNG or DNmt could predominate over the complementary attraction of nucleobases in extended sequences under physiological conditions. A means of lowering the electrostatic interactions would be to create mixed backbone ODN analogues in which strands would consist of mixed sequences of positive and negative linkers or positive and neutral linkers. We have reported[10] the synthesis of DNG/DNA chimeras having mixed anionic $-O-(PO_2^-)-O-$ and cationic $-NH-C(=NH_2^+)-NH-$ linkers.

It occurred to us that positive charges could be placed directly on the backbone of PNA by interjecting DNG or DNmt monomers into the PNA sequence. The characteristics of DNG, DNG/DNA chimera, DNmt, and PNA helical structures suggested to us that the synthesis and investigation of DNG/PNA chimeric oligos (Scheme 1) is warranted.[31] It was anticipated that placement of spaced DNG positive charges in the PNA structure would increase the rate constant for association with DNA and RNA.[32] The configurational and conformational restraints about the glycosidic bond provided by the presence of deoxyribose sugar in DNG/PNA chimeras can exert a strong orientational preference in binding with complementary DNA and RNA. The positive charges in DNG/PNA chimeras may provide more solubility in aqueous medium, inhibit self-aggregation of PNA, and enhance cell membrane permeability. In this paper, we report on the synthesis of a DNG/PNA dimer and the fully automated solid-phase synthesis of DNG/PNA chimeras and their binding properties with complementary DNA.

## Experimental Section

**Materials.** Oligonucleotides were synthesized by Sigma-Genosys. Electrophoretic reagents (acrylamide, *N*,*N*′-methylenebisacrylamide, ammonium persulfate) were from Bio-Rad, and *N*,*N*,*N*′,*N*′-tetramethylethylenediamine (TEMED) was from Boehringer Mannheim. T4 polynucleotide kinase was purchased from New England Biolabs, and [$\gamma$-$^{32}$P]ATP was from Amersham.

**General.** $^1$H and $^{13}$C NMR spectra were recorded, using Varian 400 and 100 MHz respectively, chemical shifts are reported in $\delta$ (ppm). Compounds **4**, **7**, and **1** contain tertiary amide bonds, and NMR shows

(23) Gangamani, B. P.; Kumar, V. A.; Ganesh, K. N. *Biochem. Biophys. Res. Commun.* **1997**, *240*, 778−782.
(24) Hyrup, B.; Egholm, M.; Buchardt, O.; Nielsen, P. E. *Bioorg. Med. Chem. Lett.* **1996**, *6*, 1083−1088.
(25) Koch, T.; Wittung, N. P.; Jorgensen, M.; Larsoon, C.; Buchardt, O.; Stanley, C. J.; Norden, B.; Nielsen, P. E.; Orum, H. *Tetrahedron Lett.* **1995**, *38*, 6933−6936.
(26) Uhlmann, E.; Will, D. W.; Breipohl, G.; Langer, D.; Ryte, A. *Angew. Chem., Int. Ed. Engl.* **1996**, *35*, 2632−2635.
(27) Haaima, G.; Lohse, A.; Buchardt, O.; Nielsen, P. E. *Angew. Chem., Int. Ed. Engl.* **1996**, *35*, 1939−1942.
(28) Gangamani, B. P.; Kumar, V. A.; Ganesh, K. N. *Tetrahedron* **1999**, *55*, 177−192.
(29) Blasko, A.; Dempcy, R. O.; Minyat, E. E.; Bruice, T. C. *J. Am. Chem. Soc.* **1996**, *118*, 7892−7899.
(30) Blasko, A.; Minyat, E. E.; Dempcy, R. O.; Bruice, T. C. *Biochemistry* **1997**, *36*, 7821−7831.
(31) Barawkar, D. A.; Bruice, T. C. *J. Am. Chem. Soc.* **1999**, *121*, 10418−10419.
(32) Demidov, V. V.; Frank-Kamenetskii, M. D.; Nielsen, P. E. *Biol. Struct. Dyn.* **1995**, 129−134.

two rotational isomers in the ratio 2:1, which are indicated as ma for major and mi for minor. Mass spectra were obtained using FAB. Thin-layer chromatography was carried out on aluminum-backed silica gel 60 ($F_{254}$) 0.25 mm plates (Merck). Column chromatography was performed using silica gel 230−400 mesh from ICN. DNG/PNA chimeras were synthesized using a Pharmacia GA Plus synthesizer and were purified by RP-HPLC.

**Thermal Denaturation and Circular Dichroism Studies.** The concentrations of DNG/PNA chimeras were determined using the extinction coefficients, calculated according to nearest neighbor approximation for the DNA. All melting experiments were conducted in 10 mM $Na_2HPO_4$, 100 mM NaCl, pH 7.1. The concentration of each oligonucleotide strand was 3 $\mu$M. The solutions were heated to 95 °C for 5 min and allowed to cool to room temperature slowly before being stored at 4 °C overnight. UV measurements were carried out at 260 nm on a Cary 1E UV/vis spectrophotometer, using 1 cm path length quartz cuvettes at a heating or cooling rate of 0.2 °C/min over the range of 15−90 °C. Melting temperatures were taken as the temperature of half-dissociation and were obtained from first derivative plots. The $T_m$ values are accurate to ±0.5 °C over reported values. Circular dichroism specters were recorded on an AVIV 202 spectrophotometer equipped with a Peltier heating arrangement. The buffer used was 10 mM $Na_2HPO_4$, pH 7.1, and the total sample concentration was 2.5 $\mu$M. Scans were taken at 15 °C from 350 to 210 nm with a data point obtained at every 1 nm using a 1 mm cell. Each spectrum is an average of five scans and smoothed using a 15-point exponential fitting alogorithm.

**Stoichiometry of Binding.** The stoichiometry of binding was determined by the method of continuous variation.[33] Solutions containing the different molar ratios of DNG/PNA **10** or PNA **13** and complementary DNA **15** were heated to 90 °C and allowed to cool slowly to 15 °C. The pH was maintained at 7.1 with 10 mM $Na_2HPO_4$ buffer while the ionic strength was held constant with 100 mM NaCl. The absorbance of each solution at 260 nm (15 °C) was measured with a Cary 1E UV/vis spectrophotometer.

**Preparation and End-Labeling of Oligonucleotides.** The oligonucleotides were purified by 12% denaturing polyacrylamide gel electrophoresis. The 5′ end-labeled single-stranded oligonucleotides were obtained by incubating the 1 $\mu$M oligonucleotides with 5 units of T4 polynucleotide kinase and [$\gamma$-$^{32}$P]ATP at 37 °C for 1 h. The labeled strand was then annealed with 1.3-fold of the complementary strand.

**Gel Mobility-Shift Assay.** Various concentrations of DNG/PNA or PNA were incubated with 0.005 $\mu$M duplexed oligonucleotides in 40 $\mu$L of a reaction buffer (10−20 mM $KHPO_4$, 0.1 mM $ZnCl_2$, pH 7.4) at either 37 °C or room temperature. The bound complex was separated from free DNA on an 8% native polyacrylamide gel.

**S1 Nuclease Cleavage Assay.** Various concentrations of DNG/PNA or PNA were incubated with 0.005 $\mu$M duplexed oligonucleotides in a reaction buffer (10 mM $KHPO_4$, 0.1mM $ZnCl_2$, pH 7.4) at 37 °C for 60 min, before 0.4 unit of S1 nuclease was added to the reaction mixtures. The enzyme cleavage reaction was continued for 5 min and quenched by the addition of 160 $\mu$L of a solution containing 6 mM EDTA, 0.3 M sodium acetate, and 2 $\mu$g of glycogen, followed by ethanol precipitation. The samples were loaded onto a 12% denaturing polyacrylamide gel and electrophoresed at 1600 V for 3 h.

**Imaging and Quantification.** A phosphor screen was exposed to the dried gels. Imaging and quantification were performed by a PhosphorImager using ImagQuaNT software from Molecular Dynamics.

**Synthesis: *N*-Trichloroethoxycarbonyl-*N*′-((aminoethyl)-*N*-(thyminyl-*N*(1)acetyl)-glycine ethyl ester)thiourea (4).** To Boc-protected amine **2** (5 gm, 12.2 mmol) was added trifluoroacetic acid (25 mL). The reaction mixture was kept stirring at room temperature for 45 min, concentrated under reduced pressure to an oil **3**, coevaporated with toluene, and then triturated with ether and dried under vacuum. This compound **3**, was used further without any purification. Compound **3** (3.7 gm, 11.8 mmol) was taken into anhydrous dichloromethane (100 mL) and TEA (8.5 mL, 59 mmol) and cooled in an ice bath. To this solution trichloroethoxycarbonylisothiocyanate[34] was added dropwise, and stirring was continued for 30 min in an ice bath. Water (100 mL) was added to the reaction mixture followed by extraction with $CH_2Cl_2$ (250 mL), and the organic layer was dried over $Na_2SO_4$ and evaporated to a foam. This was purified on a silica gel column equilibrated with $CH_2Cl_2$, and compound **4** was eluted at 5% MeOH. Yield was 4.54 gm (68.5%). TLC (9:1, $CH_2Cl_2$:MeOH) $R_f = 0.65$; $^1$H NMR (400 MHz, DMSO-$d_6$) $\delta$ (ppm) 1.2 ma and 1.25 mi (t, 3H, $\underline{CH_3}CH_2$), 1.75 ma and 1.78 mi (s, 3H, Thy-$\underline{CH_3}$), 3.55 mi and 3.65 ma (t, 2H, $\underline{CH_2}CH_2NCS$), 3.7 mi and 3.85 ma (q, 2H, $CH_2\underline{CH_2}NCS$), 4.05 ma and 4.35 mi (s, 2H, $N\underline{CH_2}COOEt$), 4.1 ma and 4.2 mi (q, 2H, $CH_3\underline{CH_2}$), 4.5 mi and 4.65 ma (s, 2H, $N\underline{CH_2}CON$), 4.95 mi and 5.0 ma (s, 2H, $\underline{CH_2}CCl_3$), 7.2 mi and 7.3 ma (s, 1H, Thy-H6), 9.75 mi and 9.95 ma (t, 1H, $CH_2\underline{NH}CS$), 11.3 (s, 1H, Thy-N3H), 11.5 and 11.6 (2× s, 1H, NHCS).). $^{13}$C NMR (100 MHz, $CDCl_3$) $\delta$ (ppm) 11.9 (mi) and 12 (ma), 14, 24.4 (ma) and 25.3 (mi), 33.3, 42.6 (mi) and 42.7 (ma), 45.2 (ma) and 45.5 (mi), 47.5 (ma) and 47.7 (mi), 48.2 (ma) and 48.8 (mi), 60.7 (ma) and 61.2 (mi), 73.6 (mi) and 73.8 (ma), 95.1, 108 (ma) and 108.2 (mi,), 141.9 (mi) and 142.1 (ma), 150.8 (mi) and 150.9 (ma), 151.5 (ma) and 151.6 (mi), 164.42 (mi) and 164.47 (ma), 167.3 (mi) and 167.9 (ma), 169.2 (ma) and 169.5 (mi), 179.5 (mi) and 179.8 (ma). IR (KBr pellet) 3390, 3310, 3040, 1716, 1640, 1525, 1243, 1048. HRMS (FAB) *m*/*z* $(M + H)^+$ 546.0383, calcd for $C_{17}H_{22}N_5O_7SCl_3$, 545.0305.

***N*-trichloroethoxycarbonyl-*N*′-((aminoethyl)-*N*-(thyminyl-*N*(1)-acetyl)-glycine ethyl ester)-*N*″-(5′-*N*-MMTr-3′,5′-dideoxythymidine)-guanidine (7).** To a solution of **4** (3.5 gm, 6.4 mmol) and 5′-N-MMTr-3′-amino-3′,5′-dideoxythymidine (**6**) (3.28 gm, 6.4 mmol) in anhydrous DMF (75 mL) was added anhydrous diisopropylethylamine (3.3 mL, 19.2 mmol) and $HgCl_2$ (2.08 gm, 7.68 mmol). The reaction mixture was allowed to stir overnight, whereupon a black precipitate of $Hg_2S$ was observed. The reaction was monitored by TLC and filtered over Celite, and the filtrate was evaporated to dryness under reduced pressure, resulting in a oily residue. This oil was then purified by silica gel column chromatography using a $CH_2Cl_2$:MeOH solvent system. Pure compound elutes at 6% MeOH. Yield was 4.6 gm (71%). TLC ($CH_2Cl_2$:MeOH, 9:1) $R_f = 0.55$; $^1$H NMR (400 MHz DMSO-$d_6$) $\delta$ (ppm) 1.15 ma and 1.25 mi (t, 3H, $\underline{CH_3}CH_2$), 1.75 (s, 6H, 2× Thy-$CH_3$), 2.2−2.35 (br m, 4H, H2′,2″ and H5′,5″), 2.95 (br m, 1H, H3′), 3.4−3.65 (br m, 3H, H4′ and $\underline{CH_2}CH_2NH$), 3.7 (s, 3H, $-OCH_3$), 3.9 (m, 2H, $CH_2\underline{CH_2}NH$), 4.1 ma and 4.4 mi (s, 2H, $N\underline{CH_2}COOEt$), 4.15 ma and 4.25 (q, 2H, $CH_3\underline{CH_2}$), 4.5−4.85 (3× s, 4H, $\underline{CH_2}CCl_3$ and $N\underline{CH_2}CON$), 6.1 (t, 1H, H1′), 6.8−7.45 (m, 16H, aromatic and Thy-H6), 8.75−8.9 (2 br s, 1H, $CH_2CH_2\underline{NH}$), 11.2−11.45(3× s, 3H, 2× Thy-N3H and C3′-NH). $^{13}$C NMR (100 MHz, $CDCl_3$) $\delta$ (ppm) 12.3, 12.4, 12.5, 14.1, 14.2, 25, 25.7, 31.5, 33.9, 36.6, 49, 55.3, 61.9, 70.4, 74.5, 74.8, 96.1, 110.7, 113.3, 126.4, 127.1, 127.8, 128.6, 129.3, 129.9, 141.1, 146.1, 150.9, 151.6, 158, 162.1, 162.7, 164.1, 164.7, 167.7, 169.7. IR (KBr pellet) 3386, 3313, 3025, 1720, 1615, 1556, 1315, 1055. HRMS (FAB) *m*/*z* $(M + H)^+$ 1024.2930, calcd for $C_{47}H_{52}N_9O_{11}Cl_3$, 1023.2857.

***N*-Trichloroethoxycarbonyl-*N*′-((aminoethyl)-*N*-thyminyl-*N*(1)-acetyl)-glycine)-*N*″-(5′-*N*-MMTr-3′,5′-dideoxythymidine)guanidine (1).** Compound **7** (1.3 gm, 1.26 mmol) was dissolved in 9:1 dioxane:$H_2O$ (20 mL) and was cooled in an ice bath. To this, 1 M aqueous NaOH was added dropwise until pH 11 was obtained. The reaction was stirred for 1 h and monitored by TLC, and the solution was adjusted to pH 5 by dropwise addition of 1 M aqueous $KHSO_4$. The product was extracted into dichloromethane, and the organic layer was dried over $Na_2SO_4$ and evaporated in vacuo. This was further purified by silica gel column chromatography, which gave white foam as a product. Yield was 1 gm (79.3%). TLC ($CH_2Cl_2$:MeOH, 9:1) $R_f = 0.35$; $^1$H NMR (400 MHz DMSO-$d_6$) $\delta$ (ppm) 1.55−1.95 (4× s, 6H, 2× Thy-$CH_3$), 2.15−2.45 (br m, 4H, H2′,2″ and H5′,5″), 2.85 (br m, 1H, H3′), 3.1 (m, 1H, H4′), 3.3−3.5 (br m, 2H, $\underline{CH_2}CH_2NH$), 3.65−4.0 (m, 5H, $CH_2\underline{CH_2}NH$ and $-OCH_3$), 4.2−4.9 (m, 6H, $N\underline{CH_2}COOH$, $\underline{CH_2}CCl_3$ and $N\underline{CH_2}CON$), 6.2 (t, 1H, H1′), 6.8−7.5 (m, 16H, aromatic and Thy-H6), 8.2, 8.85, 8.95, 9.3, 11.15 and 11.3 (5× s, 5H, guanidinium NH and Thy-N3H). $^{13}$C NMR (100 MHz, $CDCl_3$) $\delta$ (ppm) 8.9, 12.3, 12.6, 45.4, 55.2, 70.3, 74.7, 83.7, 96.3, 110.2, 113.2, 126.3, 127.9, 128.6, 129.9, 138.2, 141.5, 146.4, 151.8, 157.9, 160.4, 162, 164.3, 164.8, 169.3, 173.6. HRMS (FAB) *m*/*z* $(M + H)^+$ 996.2617, calcd for $C_{45}H_{48}N_9O_{11}Cl_3$, 995.2538.

(33) Job, P. *Ann. Chim.* **1928**, *9*, 113−203.

(34) Wang, S. S.; Magliocco, L. G. U.S. Patent, American Cyanamide Company, 1993, 5,194,673.

**Chart 1**

**9** $H_3N$-t t t t T*t t t t t-L

**10** $H_3N$-T*t t t t t t t T*t-L

**11** $H_3N$-t t t T*t T*t t t t-L

**12** $H_3N$-T*t t t T* t t t T*t-L

**13** $H_3N$-t t t t t t t t t t-L

**14** $H_3N$-t t t t t t t t t t-Lys-$NH_2$

**15** 5'-A A A A A A A A A A-3'

**16** 5'-A A A A G A A A A A-3'

L = HN-$(CH_2)_6$-OH

* indicates guanidinium linkage

Upper and lower cases represent nucleobases and PNA units in sequences respectively.

**Solid-Phase Synthesis of DNG/PNA Chimeras and Purification.** Synthesis of DNG/PNA chimeras **9**−**12** and PNA **13** (Chart 1) were carried out at a 1 $\mu$mol scale using MMTr-protected hexyl succinyl-amidopropyl CPG as solid support.[35] For incorporation of DNG/PNA unit dimer **1** (Scheme 2), and for incorporation of a normal PNA unit in DNG/PNA chimeras, monomer **8** was used. The monomer **8** was synthesized by using a literature method.[36] The synthesis was performed on a Pharmacia GA Plus instrument. The synthesis cycle consisted of the following steps: (i) deprotection of MMTr group (5% trichloroacetic acid in $CH_2Cl_2$, 2.5 mL/min, 3 min), (ii) neutralization (0.3 M *N*-ethylmorpholine in DMF, 2.5 mL/min, 1 min), (iii) coupling (150 $\mu$L of 0.3 M monomer **8** or dimer **1** in DMF, 100 $\mu$L of 0.3 M NEM and 200 $\mu$L of 0.3 M PyBOP with a coupling time of 45 min), and (iv) capping (A: 10% acetic anhydride/10% lutidine in THF, B: 16% *N*-methyl imidazole in THF, 1 mL/min, 1 min).

After synthesis was complete, oligomers were cleaved from the solid support using 30% $NH_4OH$ at room temperature for 3 h. This solution was then lyophilized, treated with cadmium powder in acetic acid (50 mg in 1 mL) with shaking for 90 min, and centrifuged; the supernatant was removed, and the product was lyophilized to dryness. These oligomers were then purified by RP-HPLC (10 × 250 mm, C8 silica column from Altech), Solvent A: 0.1 M TEAA, pH 7.1 and solvent B: 100% $CH_3CN$ using a gradient: 0 min, 0% B; 10 min, 0% B; 60 min, 12.5% B; 61 min, 50% B; 65 min, 50% B. The fractions collected were lyophilized, and the purity was again checked by RP-HPLC (4.6 × 250 mm, C8 silica column from Altech) with the same solvent system as above, using the gradient: 0 min, 0% B; 5 min, 0% B; 65 min, 15% B; 66 min, 50% B; 71 min, 50% B.

## Results and Discussion

The solid-phase synthesis of DNG/PNA chimeras involves nucleosides and PNA monomers. The usual *tert*-butoxycarbonyl protection of PNA N-termini and heterocyclic amino-protecting groups requires strong acidic (TFA treatment) condition, for deprotection and cleavage of PNA from solid support. Under these conditions, during synthesis of mixed base sequences, the nucleoside part of DNG/PNA chimeras can rapidly depurinate. Thus, protecting groups which can be removed under mild conditions are required. For the synthesis of DNG/PNA chimeras, the DNG/PNA dimer **1** (Scheme 2) was prepared. The 5′-amino group of dimer **1** is protected by monomethoxytrityl. This temporary protecting group can be removed after each solid-phase coupling reaction by mild acid treatment. We have previously used this strategy for the synthesis of DNG/DNA chimeras.[10]

**Scheme 2**[a]

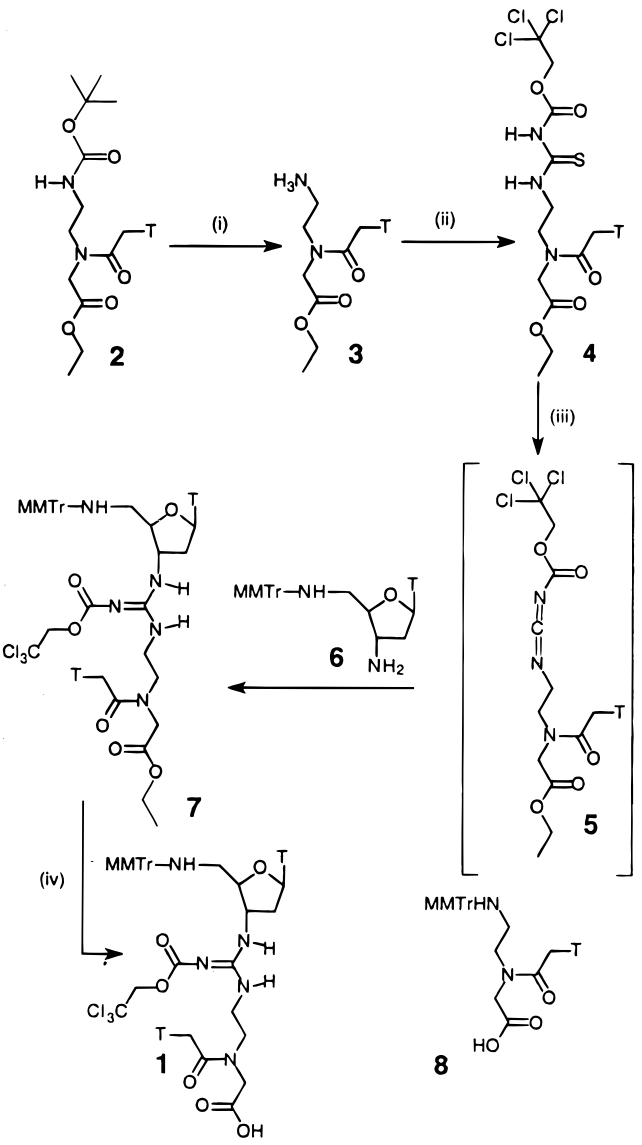


[a] (i) TFA, (ii) $Cl_3CCH_2OCONCS$, $CH_2Cl_2$/TEA, (iii) $HgCl_2$, DMF/DIPEA, (iv) NaOH, dioxane/water

The guanidinium linkage of dimer **1** was protected with a trichloroethoxy carbamate[37] and it remained protected throughout the synthesis of DNG/PNA chimeras (i.e., a permanent protecting group). The synthesis of dimer **1** involved (Scheme 2) condensation of the 3′-amino group of 5′-NH-monomethoxytrityl-3′-amino-5′,3′-dideoxythymidine **6** with in situ generated carbodiimide **5**, obtained from reaction of the protected thiourea **4** with mercury(II) in the presence of triethylamine in DMF,[10,37] to give **7**, followed by ester hydrolysis in dioxane/$H_2O$/NaOH. The protected thiourea **4** was synthesized from **2** (Scheme 2). The compound **2** was synthesized according to a literature method.[38] The protected PNA monomer **2**, upon treatment with TFA, gave the free amine **3**. The free amine **3**, upon treatment with trichloroethoxycarbonylisothiocyanate, gave protected thiourea **4**. The electron-withdrawing nature of the trichloroethoxycarbonyl group on the thiourea of **4** activates the carbodiimide

(35) Will. D. W.; Breipohl, G.; Lagner, D.; Knolle, J.; Uhlmann, E. *Tetrahedron* **1995**, *51*, 12069−12082.

(36) Breipohl, G.; Will, D. W.; Peuman, A.; Uhlmann, E. *Tetrahedron* **1997**, *53*, 14671−14686.

(37) Barawkar, D. A.; Linkletter, B.; Bruice, T. C. *Bioorg. Med. Chem. Lett.* **1998**, *8*, 1517−1520.

(38) Finn, P. J.; Gibson, N. J.; Fallon, R.; Hamilton, A.; Brown, T. *Nucleic Acids Res.* **1996**, *24*, 3357−3363.

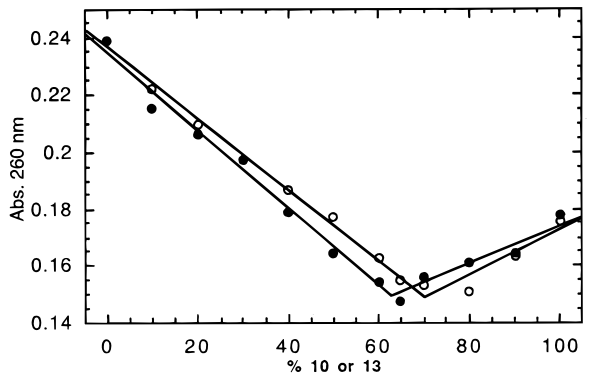


**Figure 1.** Job's plot of triplexes (●) [(**10**)$_2$·**15**] and (○) [(**13**)$_2$·**15**].

intermediate **5**, facilitating the attack by the 3′-amine of **6**. This carbamate group further acts as a protecting group of the resulting guanidinium linkage of DNG/PNA dimer **1**. The LCAA/CPG solid support,[35] cleavable by ammonia treatment, was used. This solid support utilizes an aminohexyl spacer and a base-cleaveable succinyl linker attached to LCAA-CPG. As a result of this, DNG/PNA chimeras have hydroxyhexylamides at C-termini.

The guanidinium linkage was incorporated into DNG/PNA chimeras **9**−**12** (Chart 1) by using a Pharmacia GA Plus synthesizer, which was programmed for peptide coupling reactions with 45 min of coupling time. For incorporation of DNG/PNA units into a chimera, dimer **1** was used, while for PNA units, **8** was used as a monomer. The coupling reagent used was PyBop in DMF/NEM.[35] Each coupling was followed by a capping reaction of truncated oligomers. After completion of synthesis, oligomers were cleaved from solid support by $NH_4$-OH treatment such that the resulting DNG/PNA chimeras **9**−**12** and PNA **13** possess hydroxyhexylamides at C-termini. The DNG/PNA chimeras were then treated with cadmium powder in acetic acid, which deprotects guanidinium groups[39] and the terminal MMTr. The DNG/PNA chimeras **9**−**12** were then purified by RP-HPLC. The purity of DNG/PNA chimeras was further checked on an analytical RP-HPLC column. DNG/PNA chimeras **9**−**12** have retention times of 26.5, 27.6, 27.3, and 32.3 min, respectively. FAB MS analysis of purified DNG/PNA chimera $H_2N$−t T ∗ t t−L ($C_{50}H_{73}N_{18}O_{16}$ 1182.24) indicated the expected mass.

**The Binding of the DNG/PNA Chimeras 9−12 with complementary DNA.** The chimeras **9**−**12** have one guanidinium linkage centrally placed **9** (Chart 1), two guanidinium linkages, one each at both termini **10**, two guanidinium linkages centrally placed **11**, two guanidinium linkages, one each at both termini and one in the center **12**. The stoichiometry of binding of the DNG/PNA chimeras **9**−**12** to DNA **15** was determined by the continuous variation method[33] and found to be 2:1 indicating formation of [(DNG/PNA)$_2$·DNA] triplexes (Figure 1). Relative stability of [(PNA)$_2$·DNA] and [(DNG/PNA)$_2$·DNA] triplexes were determined by comparing their $T_m$ values, which were obtained from UV-melting curves. The PNA **13** does not have a positively charged lysine amide at the C-terminus, and thus the [(PNA)$_2$·DNA] triplex [(**13**)$_2$·**15**] gave a lower $T_m$ (54.5 °C) than that for the literature report for PNA $T_{10}$ with DNA $dA_{10}$ ($T_m$, 72 °C).[16] Examination of Table 1 shows that the [(DNG/PNA)$_2$·DNA] triplexes composed of DNG/PNA chimeras **9**, **11**, and **12**, containing guanidinium at internal sites, with DNA **15** have lower melting temperatures

(39) Hancock, G.; Galpin, I. J.; Morgan, B. A. *Tetrahedron Lett*. **1982**, *23*, 249−252.

**Table 1**

| exp. no. | complex | $T_m$ (°C) | hypochromicity (%) |
|---|---|---|---|
| 1 | (**13**)$_2$·**15** | 54.5 | 17.8 |
| 2 | (**9**)$_2$·**15** | 29.5 | 27.0 |
| 3 | (**10**)$_2$·**15** | 52.5 | 25.4 |
| 4 | (**11**)$_2$·**15** | 25.5 | 15.8 |
| 5 | (**12**)$_2$·**15** | 25.5 | 13.7 |
| 6 | (**13**)$_2$·**16** | 38.5 | - |
| 7 | (**10**)$_2$·**16** | 39.5 | - |

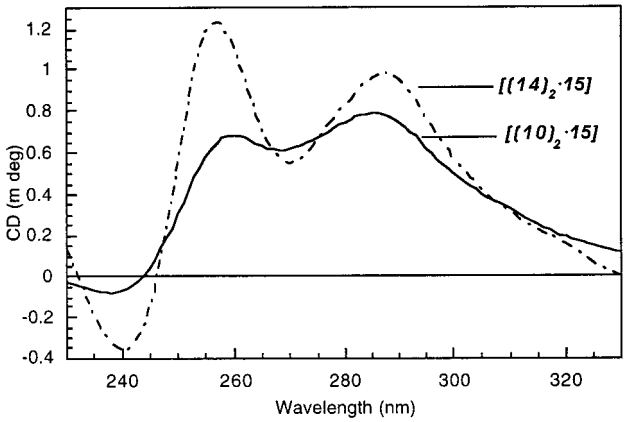


**Figure 2.** CD spectrum of triplexes [(**10**)$_2$·**15**] and [(**14**)$_2$·**15**].

than the [(PNA)$_2$·DNA] triplex [(**13**)$_2$·**15**]. This may be due to unfavorable structural changes in the backbone of these chimeras. The $T_m$ values for [(**10**)$_2$·**15**] and **[**(**13**)$_2$·**15**] are quite similar. In DNG/PNA chimera **10** the guanidinium linkages have the greatest separation, being located at terminal positions. The CD spectrum (Figure 2) of the [(DNG/PNA)$_2$·DNA] triplex [(**10**)$_2$·**15**] is very similar to that of the [(PNA)$_2$·DNA] triplex [(**14**)$_2$·**15**] and indicates formation of a similar triple helical structure.[40] However, all [(DNG/PNA)$_2$·DNA] triplexes [(**9**−**12**)$_2$·**15**] have greater stability than the corresponding DNA·DNA triplex [$(T_{10})_2$·$dA_{10}$ ] ($T_m \approx 10$ °C). These are sought after properties. The percentage hypochromicity accompanying formation of [(DNG/PNA)$_2$·DNA] triplexes [(**9**)$_2$·**15**] and [(**10**)$_2$·**15**] exceeds that for the [(PNA)$_2$·DNA] triplex [(**13**)$_2$·**15**], indicating better base stacking in [(**9**)$_2$·**15**] and [(**10**)$_2$·**15**].

To check the sequence specificity of binding of DNG/PNA chimeras with complementary DNA, DNG/PNA chimera **10** was allowed to hybridize with DNA **16**, which contains one base mismatch in the center. The triplexes [(**13**)$_2$·**16**] and [(**10**)$_2$·**16**] exhibited 16 °C and 13 °C decreases in $T_m$ (Table 1), respectively, in comparison to fully complementary [(**13**)$_2$·**15**] and [(**10**)$_2$·**15**] triplexes. This demonstrates that binding of DNG/PNA chimera **10** with complementary DNA **15** is sequence specific and involves both Watson−Crick and Hoogsteen hydrogen bonding.

Hybridization association of DNA can be monitored by the decrease in absorbance with lowering of temperature.[41] Hysteresis is observed between heating and cooling curves because the rates of association of PNA with DNA to form either duplexes or triplexes is, at usual concentrations, slower than the rates of dissociation.[19,42] As an example, the heating and cooling curves of the [(PNA)$_2$·DNA] triplex [(**13**)$_2$·**15**] show significant hysteresis (Figure 3). By substituting deoxynucleic

(40) Kim, S. K.; Nielsen, P. E.; Egholm, M.; Buchardt, O.; Berg, R. H.; Norden, B. *J. Am. Chem. Soc.* **1993**, *115*, 6477−6481.

(41) Rougee, M.; Faucon, B.; Barcelo, M. F.; Giovannangeli, C.; Garestier, T.; Helene, C. *Biochemistry* **1992**, *31*, 9269−9278.

(42) Footer, M.; Egholm, M.; Kron. S.; Coull, J. M.; Matsudaira, P. *Biochemistry* **1996**, *35*, 10673−10679.

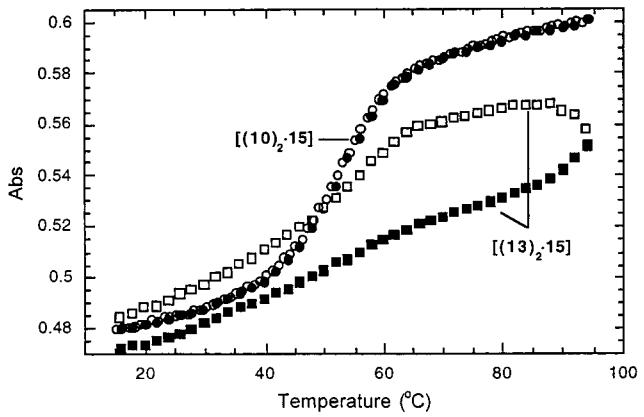


**Figure 3.** Absorbance vs temperature profiles for DNG/PNA chimera **10** and PNA **13** hybridized to DNA **15**. Dissociation (heating) curves for [(**10**)$_2$·**15**] and [(**13**)$_2$·**15**] triplexes are designated by (●) and (■), similarly (○) and (□) represent association (cooling) curves, respectively.

guanidines for terminal PNA of **13** in the structure [(**13**)$_2$·**15**] the heating and cooling curves of the resultant [(**10**)$_2$·**15**] were found to be almost overlapping (Figure 3). Clearly, the rate of association of **10** with **15** is greater than what is observed for the formation of [(**13**)$_2$·**15**] and the off and on rates for **[(10)**$_2$·**15**] are nearly equivalent.

In addition to UV melting studies with single-stranded length-matched DNA oligonucleotides, binding of DNG/PNA chimeras **9**−**12** was studied with a radio 5′ end-labeled double stranded DNA (80 mer) under more physiologic, isothermal conditions. This ds-DNA contains the dA$_{10}$ target sequence, as well as two other sites with one (5′-dA$_4$TA$_5$) and three (5′-dATA$_2$TA$_2$TA$_2$) base mismatch(es), respectively.

**Gel Mobility Shift Assay.** Binding of DNG/PNA chimeras **9**−**12** to a complementary DNA duplex containing the binding site (dA$_{10}$) was studied by a gel mobility-shift (gel retardation) assay. Our observation from thermal melting studies indicated that, the $T_m$ of [(**13**)$_2$·**15**] and [(**10**)$_2$·**15**] triplexes is quite similar (Table 1), but the results of the gel retardation assay (Figure 4), under isothermal condition, show that chimera **10** binds to duplex DNA at 2 $\mu$M concentration, while the results for PNA **13** with no lysine amide on the C-terminus show binding to only a very little extent. This clearly indicates that placing two guanidinium linkages, one each at both termini of PNA as in **10**, enhances the binding of PNA to duplex DNA target under isothermal conditions. As expected, this binding was found to be dependent on ionic strength, and there was no binding when 100 mM KCl was added to these solutions.

**Strand Invasion.** To determine whether DNG/PNA chimeras bind with ds-DNA by [DNG/PNA·(DNA)$_2$] triple helix formation or by strand invasion of ds-DNA resulting in [(DNG/PNA)$_2$·DNA] triplex with accompanying D-loop, S1 nuclease cleavage protection analysis was performed. DNG/PNA **10** and PNA **14**, with lysinecarboxamide on the C-terminus, invade ds-DNA (Figure 5) by displacing the nonsequence complementary DNA single strand, which then is a substrate for S1 nuclease cleavage. The results indicate that, after binding of chimera **10** to fully complementary target sequence, all thymines of binding site (dA$_{10}$:T$_{10}$) were specifically attacked by S1 nuclease, similar to results with PNA **14**. Introduction of one or three mismatches into DNA target sites for **10** and **14** significantly and progressively reduces S1 cleavage products yields. These results clearly indicate that DNG/PNA chimera **10** binds to ds-DNA under isothermal conditions by sequence-specific strand invasion, similar to PNA **14**. DNG/PNA chimeras **11** and **12** also showed similar binding (data not shown) but bind less well.

**Kinetics of Binding.** To study the kinetics of binding of chimera **10** and PNA **14**, a gel retardation assay was used. The radioactively labeled ds-DNA was allowed to complex with chimera **10** and PNA **14** for different times (Figure 6A), and then complexes were separated from unbound ds-DNA by electrophoresis. Autoradiographic quantification of the bands provided the percentage of the bound complexes. Figure 6B clearly shows that DNG/PNA chimera **10** associates at a greater rate (30 min, 75%) than PNA **14** (30 min, 58%). This is in agreement with our results obtained by UV studies.

In conclusion, we have successfully developed fully automated solid-phase synthesis chemistry for the insertion of positively charged guanidinium linkage(s) into PNA to provide DNG/PNA chimeras. The results from binding studies of DNG/PNA chimera **9**−**12** with length-matched oligo dA$_{10}$, show that

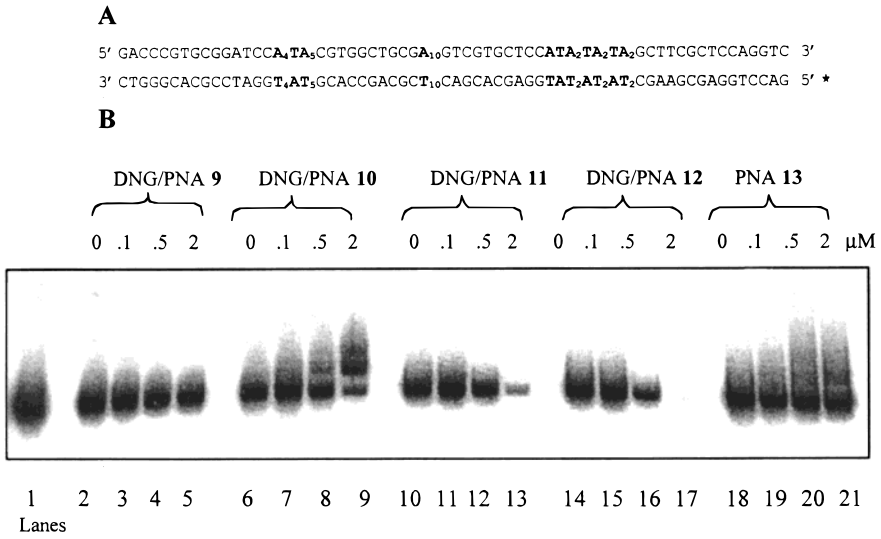


**Figure 4.** Binding of DNG/PNA chimera **9**−**12** and PNA **13** to ds-DNA. (A) The 80 bp oligonucleotide used in this study, contains the T$_{10}$ target sequence, as well as two mismatch sequences (bold phase). In all of the experiments the bottom strand was 5′ end-labeled, as indicated by an asterisk. (B) Various concentrations of DNG/PNA, as indicated in the graph, were incubated with 0.005 $\mu$M duplex oligonucleotide at either 37 °C (**10** and **13**) or room temperature (**9**, **11**, and **12**) overnight, before the samples were loaded on an 8% polyarylamide gel. Lane 1 is the control DNA without any compound. Lanes 2−5, 6−9, 10−13, 14−17, and 18−21 contain 0, 0.1, 0.5, and 2 $\mu$M of compounds, respectively.

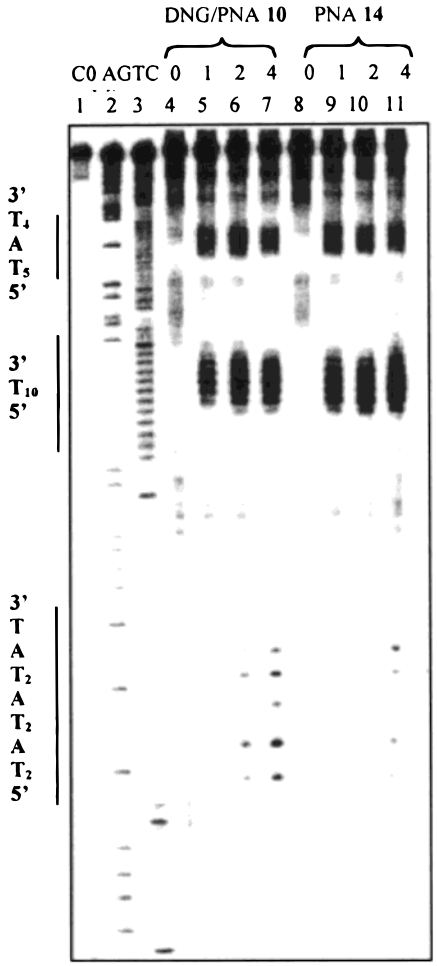


**Figure 5.** Strand displacement of DNA duplex by DNG/PNA **10** and PNA **14**. Various concentrations **10** or **14** were incubated with 0.005 $\mu$M duplex oligonucleotide at 37 °C for 60 min, before 0.4 unit of S1 was added to the reaction mixtures. The enzyme cleavage reaction continued for 5 min followed by ethanol precipitation. Lane 1 is the control without S1 nuclease. Lanes 2 and 3 contain the Maxam−Gilbert sequencing reactions. Lanes 4−7 and 8−11 contain 0, 1, 2, and 4 $\mu$M of compounds, respectively.

[(DNG/PNA)$_2$·DNA] triplexes are more stable than DNA·DNA triplexes [(T$_{10}$)$_2$·dA$_{10}$]. The insertion of guanidinium linkage(s) at internal sites of PNA results in destabilization due to possible unfavorable structural changes in the backbone. The DNG/PNA chimera **10** containing two guanidinium linkages at both termini of PNA, binds with dA$_{10}$ resulting in [(DNG/PNA)$_2$·DNA] triplex [(**10**)$_2$·**15**], which has a stability comparable to that of the [(PNA)$_2$·DNA] triplex [(**13**)$_2$·**15**]. The binding mode of DNG/PNA **10** with long ds-DNA (80 mer) is found to be strand invasion resulting in [(DNG/PNA)$_2$·DNA] triplex with the formation of D-loop. The binding of DNG/PNA chimeras with both single strand length-matched complementary DNA under thermal melt conditions and with longer double strand DNA under isothermal conditions is sequence specific. The association process of DNG/PNA **10** with single strand DNA **15** and strand invasion of longer ds-DNA under isothermal conditions is faster than the association of PNA (**13** and **14**) with the same DNA targets, as evidenced by thermal hysteresis, gel retardation, and

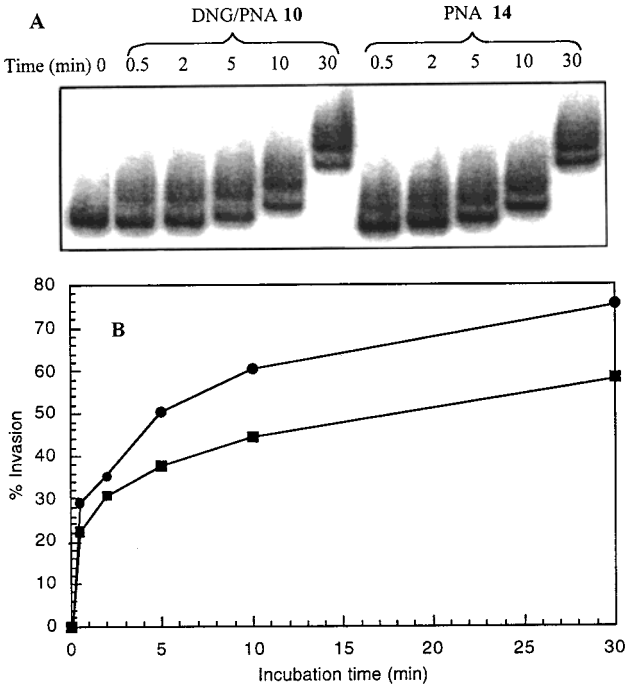


**Figure 6.** Kinetics of DNA strand displacement by DNG/PNA **10** and PNA **14**. (A) **10** or **14** (1 $\mu$M) was incubated with 0.005 $\mu$M duplex oligonucleotide at 37 °C for the time indicated in the graph, before loading on an 8% polyacrylamide gel. (B) Bands were quantitated using a phosphorimager and analyzed using ImageQuaNT software (Molecular Dynamics), (●) and (■) represent DNG/PNA **10** and PNA **14,** respectively.

S1 nuclease cleavage studies. Thus, the two important observations of sequence specific DNA strand invasion and increased hybridization association rates by DNG/PNA chimeras suggest potential utility in diagnostics, biomolecular probes, and antisense/antigene therapeutics. As chiral DNG/PNA chimeras contain configurational and conformational constraints about the glycosidic bond, they can exhibit strong orientation preferences in binding to DNA. Further work on the synthesis of mixed base sequences of DNG/PNA chimeras containing all four bases is in progress and should provide further insight on the directionality preference of DNG/PNA binding, as well as a better understanding and control of strand invasion of ds-DNA with mixed base sequences.

**Acknowledgment.** T.C.B. gratefully acknowledges support by the National Institute of Health (3 R37 DK09171-3451). Funded in part by a UC-BioStar Grant and Genelabs Technologies.

**Supporting Information Available:** $^1$H and $^{13}$C NMR spectra of compounds **4**, **6**, **7**, and **1**, mass spectra of tetramer DNG/PNA chimera H$_2$N−t T * t t−L, HPLC chromatograms of DNG/PNA chimera **9**−**12**. Autoradiograms for S1 cleavage assay on ds-DNA with DNG/PNA **9**−**12** and PNA **13** and for effect of salt concentration on strand displacement by DNG/PNA **10** (PDF). This material is available free of charge via the Internet at http://pubs.acs.org.

JA000022L